Comput Mech (2010) 45:495–511
DOI 10.1007/s00466-010-0467-3

ORIGINAL PAPER

Generalized Wishart distribution for probabilistic structural dynamics

Sondipon Adhikari

Received: 9 April 2009 / Accepted: 3 January 2010 / Published online: 23 January 2010

Abstract An accurate and efficient uncertainty quantification of the dynamic response of complex structural systems is crucial for their design and analysis. Among the many approaches proposed, the random matrix approach has received significant attention over the past decade. In this paper two new random matrix models, namely (1) generalized scalar Wishart distribution and (2) generalized diagonal Wishart distribution have been proposed. The central aims behind the proposition of the new models are to (1) improve the accuracy of the statistical predictions, (2) simplify the analytical formulations and (3) improve computational efficiency. Identification of the parameters of the newly proposed random matrix models has been discussed. Closed-form expressions have been derived using rigorous analytical approaches. It is considered that the dynamical system is proportionally damped and the mass and stiffness properties of the system are random. The newly proposed approaches are compared with the existing Wishart random matrix model using numerical case studies. Results from the random matrix approaches have been validated using an experiment on a vibrating plate with randomly attached spring-mass oscillators. One hundred nominally identical samples have been created and separately tested within a laboratory framework. Relative merits and demerits of different random matrix formulations are discussed and based on the numerical and experimental studies the recommendation for the best model has been given. A simple step-by-step method for implementing the new computational approach in conjunction with general purpose finite element software has been outlined.

S. Adhikari (✉)
School of Engineering, Swansea University,
Singleton Park, Swansea SA2 8PP, UK
e-mail: S.Adhikari@swansea.ac.uk

Keywords Unified uncertainty quantification · Random matrix theory · Wishart distribution · Model validation · Parameter identification

List of symbols

$\mathbf{f}(t)$	Forcing vector
$\mathbf{M}$, $\mathbf{C}$ and $\mathbf{K}$	Mass, damping and stiffness matrices, respectively
$\boldsymbol{\phi}_j$	Undamped eigenvectors
$\mathbf{q}(t)$	Response vector
δ_G	Dispersion parameter of $\mathbf{G}$
n	Number of degrees of freedom
$(\bullet)^T$	Matrix transposition
$\mathbb{R}$	Space of real numbers
$\mathbb{R}_n^+$	Space $n \times n$ real positive definite matrices
$\mathbb{R}^{n\times m}$	Space $n \times m$ real matrices
$\lvert\bullet\rvert$	Determinant of a matrix
etr $\{\bullet\}$	exp {Trace $(\bullet)$}
$\lVert\bullet\rVert_{\mathrm{F}}$	Frobenius norm of a matrix, $\lVert\bullet\rVert_{\mathrm{F}} = \left(\mathrm{Trace}\left((\bullet)(\bullet)^T\right)\right)^{1/2}$
$\sim$	Distributed as
Trace $(\bullet)$	Sum of the diagonal elements of a matrix
pdf	Probably density function

1 Introduction

Finite element codes implementing physics based models are used extensively for the dynamic analysis of complex systems. Laboratory based controlled tests are often performed to gain insight into some specific physics of a problem. Such tests can indeed lead to new physical laws improving the computational models. Test data can also be used to calibrate a known model. However, neither of these activities may

be enough to produce a credible numerical tool because of several types of uncertainties which exist in the physics based computational framework. Such uncertainties include, but are not limited to (1) parameter uncertainty (e.g, uncertainty in geometric parameters, friction coefficient, strength of the materials involved); (2) model uncertainty (arising from the lack of scientific knowledge about the model which is a priori unknown); (3) experimental error (uncertain and unknown errors percolate into the model when they are calibrated against experimental results). These uncertainties must be assessed and managed for credible computational predictions.

The predictions from high resolution numerical models may sometimes exhibit significant differences with the results from physical experiments due to uncertainty. When substantial statistical information exists, the theory of probability and stochastic processes offer a rich mathematical framework to represent such uncertainties. In a probabilistic setting, the data (parameter) uncertainty associated with the system parameters, such as the geometric properties and constitutive relations (i.e. Young's modulus, mass density, Poisson's ratio, damping coefficients), can be modeled as random variables or stochastic processes using the so-called parametric approach. These uncertainties can be quantified and propagated, for example, using the stochastic finite element method [8,9,15,17,20,23,25,26,28,34,40–42,49]. Recently, the uncertainty due to modelling error has received attention as this is crucial for model validation [21,22,35]. The model uncertainty problem poses serious challenges as the parameters contributing to the modelling errors are not available a priori and therefore precludes the application of a parametric approach to address such issues. Model uncertainties do not explicitly depend on the system parameters. For example, there can be unquantified errors associated with the equation of motion (linear or non-linear), in the damping model (viscous or non-viscous [3,11]), in the model of structural joints. The model uncertainty may be tackled by the so-called non-parametric method pioneered by Soize [44–46] and adopted by others [5,6,31,32].

The equation of motion of a damped n-degree-of-freedom linear dynamic system can be expressed as

$$\mathbf{M}\ddot{\mathbf{q}}(t) + \mathbf{C}\dot{\mathbf{q}}(t) + \mathbf{K}\mathbf{q}(t) = \mathbf{f}(t) \tag{1}$$

where $\mathbf{f}(t) \in \mathbb{R}^n$ is the forcing vector, $\mathbf{q}(t) \in \mathbb{R}^n$ is the response vector and $\mathbf{M} \in \mathbb{R}^{n\times n}$, $\mathbf{C} \in \mathbb{R}^{n\times n}$ and $\mathbf{K} \in \mathbb{R}^{n\times n}$ are the mass, damping and stiffness matrices respectively. In order to completely quantify the uncertainties associated with system (1) we need to obtain the probability density functions of the random matrices $\mathbf{M}$, $\mathbf{C}$ and $\mathbf{K}$. Using the parametric approach, such as the stochastic finite element method, one usually obtains a problem specific covariance structure for the elements of system matrices. The nonparametric approach [5,6,44–46] on the other hand results in a central Wishart distribution for the system matrices. In a recent paper [7] it was shown that Wishart matrix with properly selected parameters can be used for systems with both parametric uncertainty and nonparametric uncertainty. The main conclusions arising from this study were:

- Wishart random matrix distribution can be obtained either using the maximum entropy approach or using the matrix factorization approach.
- The maximum entropy approach gives a natural selection for the parameters. Through numerical examples it was shown that the parameters obtained using the maximum entropy approach may yield non-physical results. In that the 'mean of the inverse' and the 'inverse of the mean' of the random matrices can be significantly different.
- The parameters of the pdf of a Wishart random matrix obtained using the maximum entropy approach are not unique since they depend on what constraints are used in the optimization approach.
- Considering that the available 'data' is the mean and (normalized) standard deviation of a system matrix, it was shown that when the mean of the inverse equals to the inverse of the mean of the system matrices, the predictive accuracy is maximum.

The aim of this paper is to further explore the idea of proper parameter selection of Wishart matrices. Specifically, we ask the question 'what is the simplest possible Wishart random matrix model which can be used without compromising the predictive accuracy?'. The definition of 'simplest' and 'accuracy' will be explained later in the paper. The outline of the paper is as follows. In Sect. 2 dynamic response of linear stochastic systems is discussed. A brief overview of random matrix models in probabilistic structural dynamics is given in Sect. 3. The identification method of the two new random matrix model is proposed in Sect. 4. In Sect. 5 the accuracy and efficiency the proposed random matrix models are numerically verified. An experiment conducted on a vibrating plate with randomly attached sprung-mass oscillators is used to validate the proposed approach in Sect. 6. Based on the numerical and experimental studies, a step-by-step approach is outlined in Sect. 7 to apply the proposed uncertainty quantification approach.

2 Dynamic response of discrete stochastic systems

Modal analysis, originally due to Lord rayleigh [39], is the most widely used approach for linear structural dynamics. Using this approach the dynamic response of a system can be obtained by linear superposition of vibration modes. The extension of classical modal analysis to stochastic systems

requires the calculation of natural frequencies and mode-shapes which are random in nature. The efficiency and accuracy of a computational method therefore crucially dependent on the efficiency and accuracy of the calculation of random natural frequencies and mode-shapes. In this section first we transform the coupled equations of motion in the modal modal domain and then introduce uncertainty directly in natural frequencies and mode-shapes using random matrix theory. The parameter estimation and sampling of this random matrix distribution are discussed in details in later sections.

Assuming all the initial conditions are zero and taking the Laplace transform of the equation of motion (1) we have

$$\left[s^2\mathbf{M}+s\mathbf{C}+\mathbf{K}\right]\bar{\mathbf{q}}(s)=\bar{\mathbf{f}}(s) \tag{2}$$

where $(\bar{\bullet})$ denotes the Laplace transform of the respective quantities. The aim here is to obtain the statistical properties of $\bar{\mathbf{q}}(s)\in\mathbb{C}^n$ when the system matrices are random matrices. The undamped eigenvalue problem is given by

$$\mathbf{K}\boldsymbol{\phi}_j=\omega_j^2\mathbf{M}\boldsymbol{\phi}_j,\quad j=1,2,\ldots,n \tag{3}$$

where ω_j^2 and $\boldsymbol{\phi}_j$ are respectively the eigenvalues and mass-normalized eigenvectors of the system. We define the matrices

$$\boldsymbol{\Omega}=\text{diag}\left[\omega_1,\omega_2,\ldots,\omega_n\right]\quad\text{and}\quad\boldsymbol{\Phi}=\left[\boldsymbol{\phi}_1,\boldsymbol{\phi}_2,\ldots,\boldsymbol{\phi}_n\right]. \tag{4}$$

so that

$$\boldsymbol{\Phi}^T\mathbf{K}_e\boldsymbol{\Phi}=\boldsymbol{\Omega}^2\quad\text{and}\quad\boldsymbol{\Phi}^T\mathbf{M}\boldsymbol{\Phi}=\mathbf{I}_n \tag{5}$$

where $\mathbf{I}_n$ is an n-dimensional identity matrix. Using these, Eq. (2) can be transformed into the modal coordinates as

$$\left[s^2\mathbf{I}_n+s\mathbf{C}'+\boldsymbol{\Omega}^2\right]\bar{\mathbf{q}}'=\bar{\mathbf{f}}' \tag{6}$$

where and $(\bullet)'$ denotes the quantities in the modal coordinates:

$$\mathbf{C}'=\boldsymbol{\Phi}^T\mathbf{C}\boldsymbol{\Phi},\quad\bar{\mathbf{q}}=\boldsymbol{\Phi}\bar{\mathbf{q}}'\quad\text{and}\quad\bar{\mathbf{f}}'=\boldsymbol{\Phi}^T\bar{\mathbf{f}} \tag{7}$$

For simplicity let us assume that the system is proportionally [2,4,13] damped with deterministic modal damping factors $\zeta_1,\zeta_2,\ldots,\zeta_n$. Modal analysis of such systems [1,29] can be performed using real normal modes. When we consider random systems, the matrix of eigenvalues $\boldsymbol{\Omega}^2$ in Eq. (6) will be a random matrix of dimension n. Suppose this random matrix is denoted by $\boldsymbol{\Xi}\in\mathbb{R}^{n\times n}$:

$$\boldsymbol{\Omega}^2\sim\boldsymbol{\Xi} \tag{8}$$

The distribution of the random matrix $\boldsymbol{\Xi}$ will be discussed in details in Sect. 4. The steps in the rest of this section are however independent of the random matrix distribution.

Since $\boldsymbol{\Xi}$ is a symmetric and positive definite matrix, it can be diagonalized by a orthogonal matrix $\boldsymbol{\Psi}_r$ such that

$$\boldsymbol{\Psi}_r^T\boldsymbol{\Xi}\boldsymbol{\Psi}_r=\boldsymbol{\Omega}_r^2 \tag{9}$$

Here the subscript r denotes the random nature of the eigenvalues and eigenvectors of the random matrix $\boldsymbol{\Xi}$. Recalling that $\boldsymbol{\Psi}_r^T\boldsymbol{\Psi}_r=\mathbf{I}_n$, from Eq. (6) we obtain

$$\bar{\mathbf{q}}'=\left[s^2\mathbf{I}_n+s\mathbf{C}'+\boldsymbol{\Omega}^2\right]^{-1}\bar{\mathbf{f}}' \tag{10}$$

$$=\boldsymbol{\Psi}_r\left[s^2\mathbf{I}_n+2s\boldsymbol{\zeta}\boldsymbol{\Omega}_r+\boldsymbol{\Omega}_r^2\right]^{-1}\boldsymbol{\Psi}_r^T\bar{\mathbf{f}}' \tag{11}$$

where

$$\boldsymbol{\zeta}=\text{diag}\left[\zeta_1,\zeta_2,\ldots,\zeta_n\right] \tag{12}$$

The response in the original coordinate can be obtained as

$$\bar{\mathbf{q}}(s)=\boldsymbol{\Phi}\bar{\mathbf{q}}'(s)=\boldsymbol{\Phi}\boldsymbol{\Psi}_r\left[s^2\mathbf{I}_n+2s\boldsymbol{\zeta}\boldsymbol{\Omega}_r+\boldsymbol{\Omega}_r^2\right]^{-1}(\boldsymbol{\Phi}\boldsymbol{\Psi}_r)^T\bar{\mathbf{f}}(s)$$

$$=\sum_{j=1}^{n}\frac{\mathbf{x}_{r_j}^T\bar{\mathbf{f}}(s)}{s^2+2s\zeta_j\omega_{r_j}+\omega_{r_j}^2}\mathbf{x}_{r_j}. \tag{13}$$

Here

$$\boldsymbol{\Omega}_r=\text{diag}\left[\omega_{r_1},\omega_{r_2},\ldots,\omega_{r_n}\right] \tag{14}$$

$$\text{and}\quad\mathbf{X}_r=\boldsymbol{\Phi}\boldsymbol{\Psi}_r=\left[\mathbf{x}_{r_1},\mathbf{x}_{r_2},\ldots,\mathbf{x}_{r_n}\right] \tag{15}$$

are respectively the matrices containing random eigenvalues and eigenvectors of the system. The frequency response function (FRF) of the system can be obtained by substituting $s=\text{i}\omega$ in Eq. (13). In the next section we discuss the derivation of the random matrix $\boldsymbol{\Xi}$.

3 Overview of random matrix models in probabilistic structural dynamics

Recalling that $\boldsymbol{\Xi}$ is a symmetric and positive definite matrix, one can use the Wishart random matrix model [5,6,37,44–48]. Consider that a random symmetric and positive definite matrix $\mathbf{G}$ has mean $\mathbf{G}_0$ and normalized standard deviation or dispersion parameter

$$\delta_G^2=\frac{\text{E}\left[\|\mathbf{G}-\text{E}\left[\mathbf{G}\right]\|_\text{F}^2\right]}{\|\text{E}\left[\mathbf{G}\right]\|_\text{F}^2} \tag{16}$$

Suppose that $\mathbf{G}$ can be modeled by a Wishart matrix with parameters p and $\boldsymbol{\Sigma}$ so that $\mathbf{G}\sim W_n(p,\boldsymbol{\Sigma})$. The probability density function of $\mathbf{G}$ can be expressed as

$$p_\mathbf{G}(\mathbf{G})=\left\{2^{\frac{1}{2}np}\,\Gamma_n\left(\frac{1}{2}p\right)|\boldsymbol{\Sigma}|^{\frac{1}{2}p}\right\}^{-1}|\mathbf{G}|^{\frac{1}{2}(p-n-1)}$$

$$\text{etr}\left\{-\frac{1}{2}\boldsymbol{\Sigma}^{-1}\mathbf{G}\right\} \tag{17}$$

where the multivariate Gamma function is given by

$$\Gamma_n(a) = \pi^{\frac{1}{4}n(n-1)} \prod_{k=1}^{n} \Gamma\left[a - \frac{1}{2}(k-1)\right]; \quad \text{for} \quad \Re(a) > \frac{1}{2}(n-1) \tag{18}$$

We refer to the books by Muirhead [33], Eaton [14], Griko [18], Gupta and Nagar [19], Mathai and Provost [27], Tulino and Verdú [50] and Mezzadri and Snaith [30] for the derivation of the pdf in Eq. (17) and related mathematical details on random matrices.

Strictly speaking, when the parameter p is a non-integer, the probability density function in Eq. (17) is known as the matrix variate Gamma distribution, see for example, page 122 in the book by Gupta and Nagar [19]. Soize [44,45] proposed the matrix variate Gamma distribution for structural system matrices. However, when p is large as in the case of complex systems (recall that p must be more than $n+1$), the difference between the Gamma distribution and a Wishart distribution with the closest integer parameter is negligible [7]. As a result we will only consider Wishart distribution since (1) it is computationally much simpler to simulate, and (2) a very rich body of literature is available. It must be emphasized that the central Wishart distribution used here is just one of many possible symmetric random matrix distribution available in literature. Other distributions listed by Gupta and Nagar [19] such as the noncentral Wishart distribution, matrix variate beta distribution, matrix variate Dirichlet distribution and generalized quadratic-forms can be used provided their parameters can be identified easily. The parameter identification of random matrix distribution is fundamental to their effectiveness as a surrogate model to quantify uncertainty in complex dynamical systems.

In the previous works [5,6,44–46] the system matrices were separately considered as Wishart matrices. Because the matrices $\boldsymbol{\Xi}$, $\mathbf{M}$, $\mathbf{C}$ and $\mathbf{K}$ have similar mathematical properties, for notational convenience we will use the notation $\mathbf{G}$ which stands for any one of the system matrices. The parameters p and $\boldsymbol{\Sigma}$ of Wishart matrices can be obtained based on what criteria we select. For this parameter estimation problem, the 'data' consist of the 'measured' mean ($\mathbf{G}_0$) and dispersion parameter (δ_G) of a system matrix. Adhikari [7] investigated the following parameter selection methods:

1. *Parameter selection* 1: For each system matrices, one considers that the mean of the random matrix is same as the deterministic matrix and the dispersion parameter is same as the measured dispersion parameter. Mathematically this implies $\mathrm{E}[\mathbf{G}] = \mathbf{G}_0$. This condition results

$$p = n + 1 + \theta \quad \text{and} \quad \boldsymbol{\Sigma} = \mathbf{G}_0/p \tag{19}$$

where

$$\theta = \frac{1}{\delta_G^2}\{1 + \gamma_G\} - (n+1) \tag{20}$$

and

$$\gamma_G = \frac{\{\mathrm{Trace}\,(\mathbf{G}_0)\}^2}{\mathrm{Trace}\,(\mathbf{G}_0{}^2)} \tag{21}$$

This parameter selection was proposed by Soize [44,45] for $\mathbf{M}$, $\mathbf{C}$ and $\mathbf{K}$ matrices. For proportionally damped systems, this approach requires the simulation of $\mathbf{M}$ and $\mathbf{K}$ matrices.

2. *Parameter selection* 2: Here one considers that for each system matrices, the mean of the inverse of the random matrix equals to the inverse of the deterministic matrix and the dispersion parameter is same as the measured dispersion parameter. Mathematically this implies $\mathrm{E}\left[\mathbf{G}^{-1}\right] = \mathbf{G}_0{}^{-1}$. Using the theory of inverted Wishart distribution and after some simplifications one obtains

$$p = n + 1 + \theta \quad \text{and} \quad \boldsymbol{\Sigma} = \mathbf{G}_0/\theta \tag{22}$$

where θ is defined in Eq. (20). This parameter selection was proposed by Adhikari [7].

3. *Parameter selection* 3: For each system matrices, one considers that the mean of the random matrix and the mean of the inverse of the random matrix are closest to the deterministic matrix and its inverse. Mathematically this implies $\|\mathbf{G}_0 - \mathrm{E}[\mathbf{G}]\|_{\mathrm{F}}$ and $\left\|\mathbf{G}_0{}^{-1} - \mathrm{E}\left[\mathbf{G}^{-1}\right]\right\|_{\mathrm{F}}$ are minimum. This condition results:

$$p = n + 1 + \theta \quad \text{and} \quad \boldsymbol{\Sigma} = \mathbf{G}_0/\alpha \tag{23}$$

where $\alpha = \sqrt{\theta(n+1+\theta)}$ and θ is as defined in Eq. (20). This is known as the optimal Wishart distribution [5]. The rationale behind this approach is that a random system matrix and its inverse should be mathematically treated in a similar manner as both are symmetric and positive-definite matrices.

4. *Parameter selection* 4: This criteria arises from the idea that the mean of the eigenvalues of the distribution is same as the 'measured' eigenvalues of the mean matrix and the dispersion parameter is same as the measured dispersion parameter. Mathematically one can express this as

$$\mathrm{E}\left[\mathbf{M}^{-1}\right] = \mathbf{M}_0{}^{-1}, \quad \text{and} \quad \mathrm{E}[\mathbf{K}] = \mathbf{K}_0 \tag{24}$$

Based on extensive numerical studies it was shown [7] that the parameter selection 2 produces least error when the results were compared with direct Monte Carlo simulation. Even for

proportionally damped systems, following this approach, two correlated random Wishart matrices (the mass and the stiffness matrices) need to be simulated and their joint eigenvalue problem need to be solved. Here we consider the possibility of considering the matrix $\boldsymbol{\Xi}$ as the only equivalent random Wishart matrix. The motivations behind this approach are:

- Because $\boldsymbol{\Omega}^2$ is a diagonal matrix, $\boldsymbol{\Xi}$ is an uncorrelated Wishart matrix which is very easy to simulate.
- Only one matrix needs to be simulated for each sample.
- Instead of solving a generalized eigenvalue problem involving two matrices for each sample, one now needs to solve only a standard eigenvalue problem involving just one symmetric and positive definite matrix.
- Because the eigenvalues of the random system are now governed by only one random matrix, it is possible to develop further insights into the distribution of the eigenvalues.
- Due to the simplicity of the expression of the frequency response function (13), it may form the essential basis for analytical derivation of response moments using the theory of eigensolutions of Wishart matrices.

For the above points to be realized, one must (1) derive suitable parameters for the random matrix $\boldsymbol{\Xi} \sim W_n(p, \boldsymbol{\Sigma})$ from the available data, namely $\mathbf{M}_0, \mathbf{K}_0, \delta_M$ and δ_K, and (2) numerically verify that this approach results acceptable fidelity with respect to direct monte carlo simulation and if possible, experimental results. The result of the paper is devoted to address these two issues.

4 Identification of the generalized Wishart random matrix model

Because $\boldsymbol{\Xi}$ is a symmetric positive-definite matrix, $\boldsymbol{\Xi}$ can be expressed in terms of its eigenvalues and eigenvectors as $\boldsymbol{\Xi} = \boldsymbol{\Psi}\boldsymbol{\lambda}\boldsymbol{\Psi}^T$. Here $\boldsymbol{\Psi} \in \mathbb{R}^{n\times n}$ is an orthonormal matrix containing the eigenvectors of $\boldsymbol{\Xi}$, that is, $\boldsymbol{\Psi}^T\boldsymbol{\Psi} = \mathbf{I}_n$ and $\boldsymbol{\lambda}$ is a real diagonal matrix containing the eigenvalues of $\boldsymbol{\Xi}$. The Frobenius norm of the matrix λ_2^2 is given by

$$\begin{aligned}\|\boldsymbol{\Xi}\|_{\mathrm{F}}^2 &= \mathrm{Trace}\left(\boldsymbol{\Xi}\boldsymbol{\Xi}^T\right) = \mathrm{Trace}\left(\boldsymbol{\Psi}\boldsymbol{\lambda}\boldsymbol{\Psi}^T\boldsymbol{\Psi}\boldsymbol{\lambda}\boldsymbol{\Psi}^T\right)\\ &= \mathrm{Trace}\left(\boldsymbol{\Psi}^T\boldsymbol{\Psi}\boldsymbol{\lambda}\boldsymbol{\lambda}\right) = \lambda_1^2+\lambda_2^2+\cdots+\lambda_n^2 \end{aligned} \tag{25}$$

Note that the eigenvalues of $\boldsymbol{\Xi}$ are same as the eigenvalues of $\mathbf{M}^{-1}\mathbf{K}$ or $\mathbf{M}^{-1/2}\mathbf{K}\mathbf{M}^{-1/2}$. We define the matrix $\mathbf{H}$ as

$$\mathbf{H} = \mathbf{M}^{-1}\mathbf{K} \tag{26}$$

Therefore, form the definition of dispersion parameter in Eq. (16) and the expression of the Frobenius norm in Eq. (25), we can say that the dispersion parameter of $\boldsymbol{\Xi}$ is same as that of $\mathbf{H}$. The main challenge here is that the dispersion parameter of $\mathbf{H}$ needs to be obtained from dispersion parameters of $\mathbf{M}$ and $\mathbf{K}$. We propose a new approach based on the theory of inverted Wishart random matrices.

It should be note that when $\mathbf{M}$ and $\mathbf{K}$ are Wishart matrices, theoretically $\mathbf{H} = \mathbf{M}^{-1/2}\mathbf{K}\mathbf{M}^{-1/2}$ cannot be Wishart matrices. The exact distribution of such matrices may be obtained using the Jacobian associated with the non-linear transformation of Wishart matrices as discussed by Gupta and Nagar [19]. On the other hand, theoretically one can directly derive the Wishart random matrix model for the symmetric and positive definite matrix $\mathbf{H}$ using the maximum entropy approach proposed by Soize [44,45] or the matrix factorization approach proposed by Adhikari [7]. In that case the individual system matrices $\mathbf{M}$ and $\mathbf{K}$ will not be Wishart matrices. The generalized Wishart approach proposed here therefore do not strictly follow from the original Wishart matrix model of the system matrices. The approach presented here should be considered as another approximate approach derived for mathematical simplicity and computational efficiency. With this spirit, we *fit* an equivalent Wishart distribution for the matrix $\mathbf{H}$.

From the numerator of the definition of the dispersion parameter in Eq. (16) we have

$$\begin{aligned}\mathrm{E}\left[\|\mathbf{H}-\mathrm{E}[\mathbf{H}]\|_{\mathrm{F}}^2\right] &= \mathrm{E}\left[\mathrm{Trace}\left([\mathbf{H}-\mathrm{E}[\mathbf{H}]][\mathbf{H}-\mathrm{E}[\mathbf{H}]]^T\right)\right]\\ &= \mathrm{Trace}\left(\mathrm{E}\left[[\mathbf{H}^2-\mathbf{H}\,\mathrm{E}[\mathbf{H}]-\mathrm{E}[\mathbf{H}]\,\mathbf{H}-\mathrm{E}[\mathbf{H}]^2]\right]\right)\\ &= \mathrm{Trace}\left(\mathrm{E}\left[\mathbf{H}^2\right]-\mathrm{E}[\mathbf{H}]^2\right) = \mathrm{Trace}\left(\mathrm{E}\left[\mathbf{H}^2\right]\right)\\ &\quad -\mathrm{Trace}\left(\mathrm{E}[\mathbf{H}]^2\right)\\ &= \mathrm{Trace}\left(\mathrm{E}\left[\mathbf{M}^{-1}\mathbf{K}\,\mathbf{M}^{-1}\mathbf{K}\right]\right)-\mathrm{Trace}\left(\left(\mathrm{E}\left[\mathbf{M}^{-1}\mathbf{K}\right]\right)^2\right)\end{aligned} \tag{27}$$

Let us assume

$$\mathbf{M} \sim W_n(p_1, \boldsymbol{\Sigma}_1) \quad \text{and} \quad \mathbf{K} \sim W_n(p_2, \boldsymbol{\Sigma}_2) \tag{28}$$

Following Theorems 3.3.15, 3.3.15 and 3.3.17 of Gupta and Nagar [19] we have the following useful results

$$\mathrm{E}[\mathbf{K}] = p_2\boldsymbol{\Sigma}_2 \tag{29}$$

$$\begin{aligned}\mathrm{E}[\mathbf{K}\mathbf{B}\mathbf{K}] &= p_2\boldsymbol{\Sigma}_2\mathbf{B}^T\boldsymbol{\Sigma}_2 + p_2\mathrm{Trace}(\boldsymbol{\Sigma}_2\mathbf{B})\,\boldsymbol{\Sigma}_2\\ &\quad + p_2^2\boldsymbol{\Sigma}_2\mathbf{B}\boldsymbol{\Sigma}_2\end{aligned} \tag{30}$$

$$\mathrm{E}\left[\mathbf{M}^{-1}\right] = c_0\boldsymbol{\Sigma}_1^{-1} \tag{31}$$

$$\begin{aligned}\mathrm{E}\left[\mathbf{M}^{-1}\mathbf{A}\mathbf{M}^{-1}\right] &= c_1\boldsymbol{\Sigma}_1^{-1}\mathbf{A}\boldsymbol{\Sigma}_1^{-1}\\ &\quad + c_2\left[\boldsymbol{\Sigma}_1^{-1}\mathbf{A}^T\boldsymbol{\Sigma}_1^{-1} + \mathrm{Trace}\left(\mathbf{A}\boldsymbol{\Sigma}_1^{-1}\right)\boldsymbol{\Sigma}_1^{-1}\right]\end{aligned} \tag{32}$$

$$\begin{aligned}\text{and}\quad \mathrm{E}\left[\mathrm{Trace}\left(\mathbf{A}\mathbf{M}^{-1}\right)\mathrm{Trace}\left(\mathbf{B}\mathbf{M}^{-1}\right)\right]\\ = c_1\mathrm{Trace}\left(\mathbf{A}\boldsymbol{\Sigma}_1^{-1}\right)\mathrm{Trace}\left(\mathbf{B}\boldsymbol{\Sigma}_1^{-1}\right)\end{aligned}$$

$$+ c_2 \left[\text{Trace}\left(\mathbf{B}\boldsymbol{\Sigma}_1^{-1}\mathbf{A}\boldsymbol{\Sigma}_1^{-1}\right) + \text{Trace}\left(\mathbf{B}\boldsymbol{\Sigma}_1^{-1}\mathbf{A}^T\boldsymbol{\Sigma}_1^{-1}\right)\right] \tag{33}$$

Here $\mathbf{A}$ and $\mathbf{B}$ are $n \times n$ matrices and the constants c_0, c_1 and c_2 are defined as

$$c_0 = (p_1 - n - 1)^{-1}, c_1 = (p_1 - n - 2)c_2 \quad \text{and} \quad c_2 = \{(p_1 - n)(p_1 - n - 1)(p_1 - n - 3)\}^{-1} \tag{34}$$

Equations (29)–(33) and the fact that $\boldsymbol{\Sigma}_1$ and $\boldsymbol{\Sigma}_2$ are symmetric matrices will be used to derive the dispersion parameter for the $\mathbf{H}$ matrix. We use the notation

$$\mathbf{H}_0 = {\mathbf{M}_0}^{-1}\mathbf{K}_0 \tag{35}$$

Note that $\mathbf{H}_0$ is in general not the mean of the $\mathbf{H}$ matrix. Because $\mathbf{M}$ and $\mathbf{K}$ are statistically independent random matrices, we have

$$\begin{aligned}
\text{E}\left[\mathbf{M}^{-1}\mathbf{K}\,\mathbf{M}^{-1}\mathbf{K}\right] &= \text{E}\left[\mathbf{M}^{-1}\,\text{E}\left[\mathbf{K}\mathbf{M}^{-1}\mathbf{K}\right]\right] \\
&= \text{E}\left[\mathbf{M}^{-1}\left\{p_2\boldsymbol{\Sigma}_2\mathbf{M}^{-1}\boldsymbol{\Sigma}_2 + p_2\text{Trace}\left(\boldsymbol{\Sigma}_2\mathbf{M}^{-1}\right)\boldsymbol{\Sigma}_2 + p_2^2\boldsymbol{\Sigma}_2\mathbf{M}^{-1}\boldsymbol{\Sigma}_2\right\}\right] \\
&= (p_2 + p_2^2)\text{E}\left[\mathbf{M}^{-1}\boldsymbol{\Sigma}_2\mathbf{M}^{-1}\right]\boldsymbol{\Sigma}_2 + p_2\text{E}\left[\mathbf{M}^{-1}\boldsymbol{\Sigma}_2\text{Trace}\left(\boldsymbol{\Sigma}_2\mathbf{M}^{-1}\right)\right]
\end{aligned} \tag{36}$$

Taking the trace of the above equation and noting that the order of the expectation and trace operators can be interchanged we have

$$\begin{aligned}
&\text{Trace}\left(\text{E}\left[\mathbf{M}^{-1}\mathbf{K}\,\mathbf{M}^{-1}\mathbf{K}\right]\right) \\
&= (p_2 + p_2^2)\text{Trace}\left(\text{E}\left[\mathbf{M}^{-1}\boldsymbol{\Sigma}_2\mathbf{M}^{-1}\right]\boldsymbol{\Sigma}_2\right) \\
&\quad + p_2\text{E}\left[\text{Trace}\left(\boldsymbol{\Sigma}_2\mathbf{M}^{-1}\right)\text{Trace}\left(\boldsymbol{\Sigma}_2\mathbf{M}^{-1}\right)\right]
\end{aligned} \tag{37}$$

Using Eq. (32), the first term in right hand side can be obtained as

$$\begin{aligned}
&\text{Trace}\left(\text{E}\left[\mathbf{M}^{-1}\boldsymbol{\Sigma}_2\mathbf{M}^{-1}\right]\boldsymbol{\Sigma}_2\right) \\
&= \text{Trace}\left(\left(c_1\boldsymbol{\Sigma}_1^{-1}\boldsymbol{\Sigma}_2\boldsymbol{\Sigma}_1^{-1} + c_2\left[\boldsymbol{\Sigma}_1^{-1}\boldsymbol{\Sigma}_2\boldsymbol{\Sigma}_1^{-1} + \text{Trace}\left(\boldsymbol{\Sigma}_2\boldsymbol{\Sigma}_1^{-1}\right)\boldsymbol{\Sigma}_1^{-1}\right]\right)\boldsymbol{\Sigma}_2\right) \\
&= (c_1 + c_2)\text{Trace}\left(\left(\boldsymbol{\Sigma}_1^{-1}\boldsymbol{\Sigma}_2\right)^2\right) + c_2\left(\text{Trace}\left(\boldsymbol{\Sigma}_1^{-1}\boldsymbol{\Sigma}_2\right)\right)^2
\end{aligned} \tag{38}$$

Using Eq. (33), the second term in right hand side of Eq. (37) can be obtained as

$$\text{E}\left[\text{Trace}\left(\boldsymbol{\Sigma}_2\mathbf{M}^{-1}\right)\text{Trace}\left(\boldsymbol{\Sigma}_2\mathbf{M}^{-1}\right)\right] = c_1\left(\text{Trace}\left(\boldsymbol{\Sigma}_1^{-1}\boldsymbol{\Sigma}_2\right)\right)^2 + 2c_2\text{Trace}\left(\left(\boldsymbol{\Sigma}_1^{-1}\boldsymbol{\Sigma}_2\right)^2\right) \tag{39}$$

Using the notations

$$\alpha_a = \text{Trace}\left(\left(\boldsymbol{\Sigma}_1^{-1}\boldsymbol{\Sigma}_2\right)^2\right) \quad \text{and} \quad \alpha_b = \left(\text{Trace}\left(\boldsymbol{\Sigma}_1^{-1}\boldsymbol{\Sigma}_2\right)\right)^2 \tag{40}$$

and substituting Eqs. (38) and (39) into Eq. (37) we have

$$\text{Trace}\left(\text{E}\left[\mathbf{M}^{-1}\mathbf{K}\,\mathbf{M}^{-1}\mathbf{K}\right]\right) = (p_2 + p_2^2)\{(c_1 + c_2)\alpha_a + c_2\alpha_b\} + p_2\{c_1\alpha_b + 2c_2\alpha_a\} \tag{41}$$

For the second term in right-hand side of Eq. (27) we have

$$\text{E}\left[\mathbf{M}^{-1}\mathbf{K}\right] = \text{E}\left[\mathbf{M}^{-1}\right]\text{E}\left[\mathbf{K}\right] = c_0\boldsymbol{\Sigma}_1^{-1}p_2\boldsymbol{\Sigma}_2 \tag{42}$$

Therefore,

$$\begin{aligned}
\text{Trace}\left(\left(\text{E}\left[\mathbf{M}^{-1}\mathbf{K}\right]\right)^2\right) &= c_0^2p_2^2\text{Trace}\left(\left(\boldsymbol{\Sigma}_1^{-1}\boldsymbol{\Sigma}_2\right)^2\right) \\
&= c_0^2p_2^2\alpha_a
\end{aligned} \tag{43}$$

From the expressions of the dispersion parameter in Eq. (16) we have

$$\begin{aligned}
\delta_H^2 &= \frac{\text{Trace}\left(\text{E}\left[\mathbf{M}^{-1}\mathbf{K}\,\mathbf{M}^{-1}\mathbf{K}\right]\right) - \text{Trace}\left(\left(\text{E}\left[\mathbf{M}^{-1}\mathbf{K}\right]\right)^2\right)}{\text{Trace}\left(\left(\text{E}\left[\mathbf{M}^{-1}\mathbf{K}\right]\right)^2\right)} \\
&= \frac{(p_2 + p_2^2)((c_1 + c_2)\alpha_a + c_2\alpha_b) + p_2(c_1\alpha_b + 2c_2\alpha_a) - c_0^2p_2^2\alpha_a}{c_0^2p_2^2\alpha_a}
\end{aligned} \tag{44}$$

Following parameter the Sect. 2 discussed in the previous section we have

$$\boldsymbol{\Sigma}_1 = \mathbf{M}_0/\theta_M,\ p_1 = \frac{\gamma_M + 1}{\delta_M} \tag{45}$$

$$\text{and} \quad \boldsymbol{\Sigma}_2 = \mathbf{K}_0/\theta_K,\ p_2 = \frac{\gamma_K + 1}{\delta_K} \tag{46}$$

Using these and following the definition of the parameter γ in Eq. (21) one has

$$\begin{aligned}
\gamma_H &= \frac{\{\text{Trace}\,(\mathbf{H}_0)\}^2}{\text{Trace}\,(\mathbf{H}_0^2)} = \frac{\left\{\text{Trace}\left(\left(\mathbf{M}_0^{-1}\mathbf{K}_0\right)\right)\right\}^2}{\text{Trace}\left(\left(\mathbf{M}_0^{-1}\mathbf{K}_0\right)^2\right)} \\
&= \frac{\left(\text{Trace}\left(\boldsymbol{\Sigma}_1^{-1}\boldsymbol{\Sigma}_2\right)\right)^2}{\text{Trace}\left(\left(\boldsymbol{\Sigma}_1^{-1}\boldsymbol{\Sigma}_2\right)^2\right)} = \frac{\alpha_b}{\alpha_a}
\end{aligned} \tag{47}$$

Suppose $\mathbf{\Omega}_0$ is the diagonal matrix containing the undamped natural frequencies corresponding to the baseline system consisting the mass and stiffness matrices $\mathbf{M}_0$ and $\mathbf{K}_0$ respectively. Then the constant γ_H can be obtained as

$$\gamma_H = \frac{\{\text{Trace}\,(\mathbf{H}_0)\}^2}{\text{Trace}\,(\mathbf{H}_0^2)} = \frac{\left\{\text{Trace}\,\left(\mathbf{\Omega}_0^2\right)\right\}^2}{\text{Trace}\,\left(\mathbf{\Omega}_0^4\right)} = \frac{\left(\sum_j \omega_{0_j}^2\right)^2}{\sum_j \omega_{0_j}^4} \tag{48}$$

Substituting $\alpha_b = \gamma_H \alpha_a$ in Eq. (44) we have

$$\delta_H^2 = \frac{(c_2 + p_2 c_2 + c_1)\,\gamma_H + c_1 + 3\,c_2 + p_2 c_1 + p_2 c_2 - {c_0}^2 p_2}{c_0^2 p_2} \tag{49}$$

Using the expression of the constants c_0–c_2 in Eq. (34), this expression can be further simplified as

$$\delta_H^2 = \frac{\left({p_1}^2 + (p_2 - 2 - 2n)\,p_1 + (-n-1)\,p_2 + n^2 + 1 + 2n\right)\gamma_H}{p_2\,(-p_1+n)\,(-p_1+n+3)} + \frac{{p_1}^2 + (p_2 - 2\,n)\,p_1 + (1-n)\,p_2 - 1 + n^2}{p_2\,(-p_1+n)\,(-p_1+n+3)} \tag{50}$$

This equation completely defines the dispersion parameter of the generalized random matrix in closed-form.

Based on the expression of δ_H together with the 'mean matrix' $\mathbf{\Omega}_0^2$, two types of Wishart random matrix models are proposed for the generalized system matrix $\mathbf{\Xi}$:

(a) *Scalar Wishart Matrix:* In this case it is assumed that

$$\mathbf{\Xi} \sim W_n\left(p, \frac{a^2}{n}\mathbf{I}_n\right) \tag{51}$$

Considering $\text{E}\,[\mathbf{\Xi}] = \mathbf{\Omega}_0^2$ and $\delta_{\mathbf{\Xi}} = \delta_H$ the values of the unknown parameters can be obtained as

$$p = \frac{1+\gamma_H}{\delta_H^2} \quad \text{and} \quad a^2 = \text{Trace}\left(\mathbf{\Omega}_0^2\right)/p \tag{52}$$

(b) *Diagonal Wishart Matrix with different entries:* In this case it is assumed that

$$\mathbf{\Xi} \sim W_n\left(p, \mathbf{\Omega}_0^2/\theta\right) \tag{53}$$

Considering $\text{E}\left[\mathbf{\Xi}^{-1}\right] = \mathbf{\Omega}_0^{-2}$ and $\delta_{\mathbf{\Xi}} = \delta_H$ as proposed in [7] we have

$$p = n + 1 + \theta \quad \text{and} \quad \theta = \frac{(1+\gamma_H)}{\delta_H^2} - (n+1) \tag{54}$$

The samples of $\mathbf{\Xi}$ can be generated using the procedure outlined in the previous works [5,7]. The constant p needs to be approximated to the nearest integer of $n + 1 + \theta$ so that $p = [n + 1 + \theta]$. For complex engineering systems n can be in the order of several thousands or even millions. For this reason, as shown in reference [7], this approximation introduces negligible error. Now we create an $n \times p$ matrix $\widetilde{\mathbf{Y}}$ with Gaussian random numbers with zero mean and unit covariance i.e., $\widetilde{\mathbf{Y}} \sim N_{n,p}\left(\mathbf{O}, \mathbf{I}_n \otimes \mathbf{I}_p\right)$. Note $\mathbf{\Sigma} = \mathbf{\Omega}_0^2/\theta$ is a positive definite diagonal matrix. It can be factorized as $\mathbf{\Sigma} = \left[\mathbf{\Omega}_0/\sqrt{\theta}\right]\left[\mathbf{\Omega}_0/\sqrt{\theta}\right]^T$. Using this, we can obtain the matrix $\mathbf{Y}$ using the linear transformation

$$\mathbf{Y} = \mathbf{\Omega}_0 \widetilde{\mathbf{Y}}/\sqrt{\theta} \tag{55}$$

Following theorem 2.3.10 in [19] it can be shown that $\mathbf{Y} \sim N_{n,p}\left(\mathbf{O}, \mathbf{\Omega}_0^2/\theta \otimes \mathbf{I}_p\right)$. One can now obtain the samples of the Wishart random matrices $W_n\left(n+1+\theta, \mathbf{\Omega}_0^2/\theta\right)$ as

$$\mathbf{\Xi} = \mathbf{Y}\mathbf{Y}^T \tag{56}$$

Alternatively, MATLAB® command `wishrnd` can be used to generate the samples of Wishart matrices. One need to solve the symmetric eigenvalue problem for every sample

$$\mathbf{\Xi}\,\mathbf{\Psi}_r = \mathbf{\Omega}_r^2 \mathbf{\Psi}_r \tag{57}$$

The eigenvalue and eigenvector matrices $\mathbf{\Omega}_r^2$ and $\mathbf{\Psi}_r$ can then be substituted in Eq. (13) to obtain the dynamic response. These two random matrix models together with the original approach proposed by Soize [44,45] are compared in the next sections. Two numerical and one experimental case studies are considered.

5 Numerical investigations

A rectangular cantilever steel plate is considered to illustrate the application of the proposed generalized Wishart random matrices in probabilistic structural dynamics. The deterministic properties are assumed to be $\bar{E} = 200 \times 10^9\,\text{N/m}^2$, $\bar{\nu} = 0.3$, $\bar{\rho} = 7{,}860\,\text{kg/m}^3$, $\bar{t} = 3.0\,\text{mm}$, $L_x = 0.998\,\text{m}$, $L_y = 0.59\,\text{m}$. These values correspond to the experimental study discussed in the next section. The schematic diagram of the plate is shown in Fig. 1. The plate is excited by an unit harmonic force and the response is calculated at the point shown in the diagram. The plate is divided into 25 elements along the x-axis and 15 elements along the y-axis for the numerical calculations. The resulting system has 1,200 degrees of freedom so that $n = 1{,}200$. Response is calculated for the six points shown in the figure. These points correspond to location of the accelerometers used in the experimental study. Here we show results corresponding to points 1 and 2 only. Two different cases of uncertainties are considered. In the first case, it is assumed that the material properties are randomly inhomogeneous. In the second case, we consider that the plate is 'perturbed' by attaching spring-mass oscillators

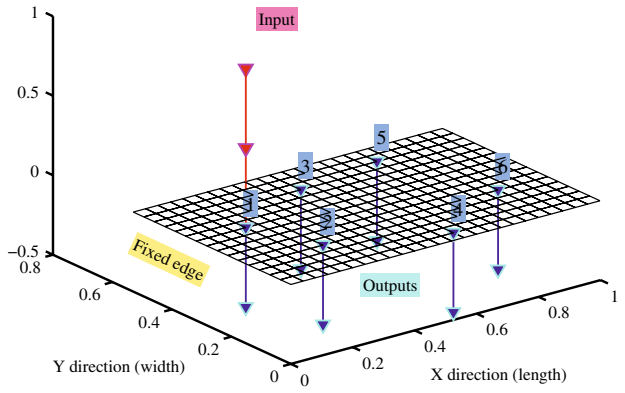

Fig. 1 Schematic diagram of a steel cantilever plate. The deterministic properties are: $\bar{E} = 200 \times 10^9\,\mathrm{N/m^2}$, $\bar{\nu} = 0.3$, $\bar{\rho} = 7{,}860\,\mathrm{kg/m^3}$, $\bar{t} = 3.0\,\mathrm{mm}$, $L_x = 0.998\,\mathrm{m}$, $L_y = 0.59\,\mathrm{m}$. A modal damping factor of 2% is assumed for all modes

at random locations. The first case corresponds to a parametric uncertainty problem while the second case corresponds to a non-parametric uncertainty problem.

5.1 Plate with randomly inhomogeneous material properties: parametric uncertainty problem

It is assumed that the Young's modulus, Poissons ratio, mass density and thickness are random fields of the form

$$E(\mathbf{x}) = \bar{E}\,(1 + \epsilon_E f_1(\mathbf{x})), \quad \nu(\mathbf{x}) = \bar{\nu}\,(1 + \epsilon_\nu f_2(\mathbf{x})) \tag{58}$$

$$\rho(\mathbf{x}) = \bar{\rho}\,\left(1+\epsilon_\rho f_3(\mathbf{x})\right) \quad \text{and} \quad t(\mathbf{x}) = \bar{t}\,(1+\epsilon_t f_4(\mathbf{x})) \tag{59}$$

The two dimensional vector $\mathbf{x}$ denotes the spatial coordinates. The strength parameters are assumed to be $\epsilon_E = 0.10$, $\epsilon_\nu = 0.10$, $\epsilon_\rho = 0.08$ and $\epsilon_t = 0.12$. The random fields $f_i(\mathbf{x}), i = 1, \ldots, 4$ are assumed to be correlated homogenous Gaussian random fields. An exponential correlation function with correlation length 0.2 times the lengths in each direction has been considered. The random fields are simulated by expanding them using the Karhunen-Loève expansion [17,36] involving uncorrelated standard normal variables. A 5000-sample Monte Carlo simulation is performed to obtain the frequency response functions (FRFs) of the system. The quantities $E(\mathbf{x})$, $\rho(\mathbf{x})$ and $t(\mathbf{x})$ are positive while $-1 \leq \nu(\mathbf{x}) \leq 1/2$ for all $\mathbf{x}$. Due to the bounded nature of these quantities, the Gaussian random field is not an ideal model for these quantities. However, due to small variability considered for these parameters, the probability that any of these quantities become non-physical is small. We have explicitly verified that all the realizations of these four random fields are physical in nature in our Monte Carlo simulation.

We want to identify which of the two Wishart matrix fitting approaches proposed here would produce highest fidelity with direct stochastic finite element Monte Carlo Simulation results. Recall that these simplified methods require simulation of only one uncorrelated Wishart random matrix. As a result, we are also interested to understand whether significant accuracy is lost when comparing these simplified methods with the original approach involving two fully correlated Wishart matrices [44,45].

From the simulated random mass and stiffness matrices we obtain $\delta_M = 0.1133$ and $\delta_K = 0.2916$. Since 2% constant modal damping factor is assumed for all the modes, $\delta_C = 0$. The *only* uncertainty related information used in the random matrix approach are the values of δ_M and δ_K. The information regarding which element property functions are random fields, nature of these random fields (correlation structure, Gaussian or non-Gaussian) and the amount of randomness are *not* used in the Wishart matrix approach. This is aimed to depict a realistic situation when the detailed information regarding uncertainties in a complex engineering system is not available to the analyst.

The predicted mean of the amplitude using the direct stochastic finite element simulation and three Wishart matrix approaches are compared in Fig. 2 for the driving-point-FRF (node number 481) and a cross FRF (node number 877). In Fig. 3 percentage errors in the mean of the amplitude of the driving-point and cross-FRF obtained using the proposed three Wishart matrix approaches are shown. Percentage errors are calculated using the direct Monte Carlo simulation results as the benchmarks. The computational cost using each of the two single uncorrelated Wishart random matrix model turns out to be about 30% less compared to the fully correlated case. The computational efficiency is likely to increase with larger system dimensions and number of samples used in the Monte Carlo simulation.

The predicted standard deviation of the amplitude using the direct stochastic finite element simulation and three Wishart matrix approaches are compared in Fig. 4 for the driving-point-FRF and the cross FRF. In Fig. 5 percentage errors in the standard deviation of the amplitude of the driving-point and cross-FRF obtained using the proposed three Wishart matrix approaches are shown. Percentage errors are calculated using the direct Monte Carlo simulation results as the benchmarks. Error in both mean and standard deviation using any one of the random matrix approaches reduce with the increase in frequency. Among the three Wishart matrix approaches discussed here, the diagonal Wishart matrix with different entries produces most accurate results across the frequency range. As expected, the scalar Wishart matrix model produces least accurate results. Note that this approach only need the simulation of one random matrix. From these results we conclude that the diagonal Wishart matrix with different entries should be used for a system with parametric uncertainty. In the next section we discuss the same system with non-parametric uncertainty.

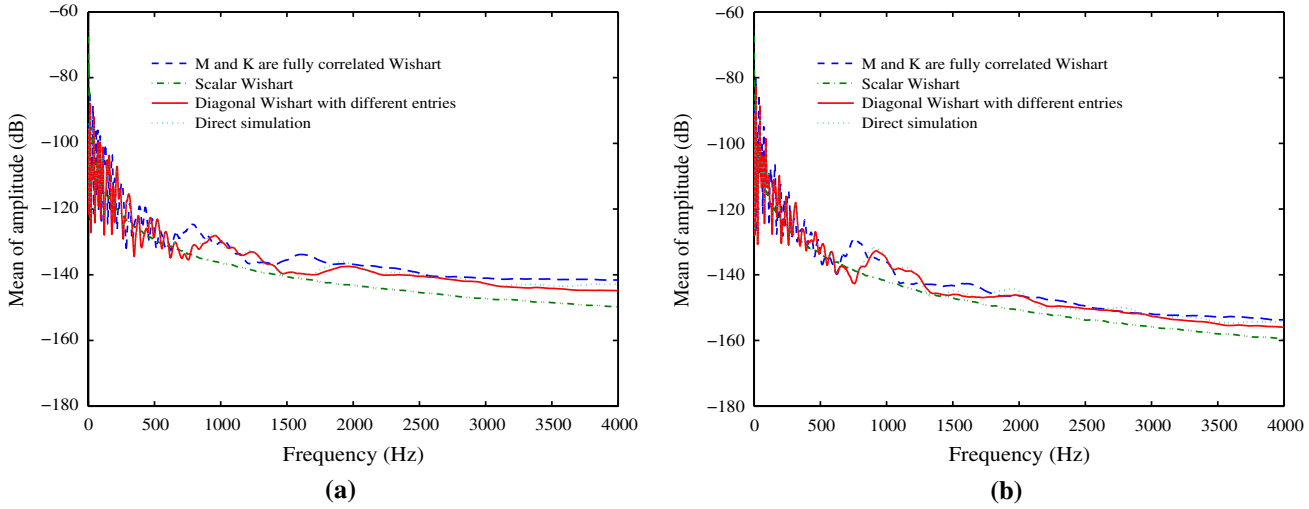

Fig. 2 Comparison of the mean of the amplitude obtained using the direct stochastic finite element simulation and three Wishart matrix approaches for the plate with randomly inhomogeneous material properties. **a** Driving-point-FRF. **b** Cross FRF

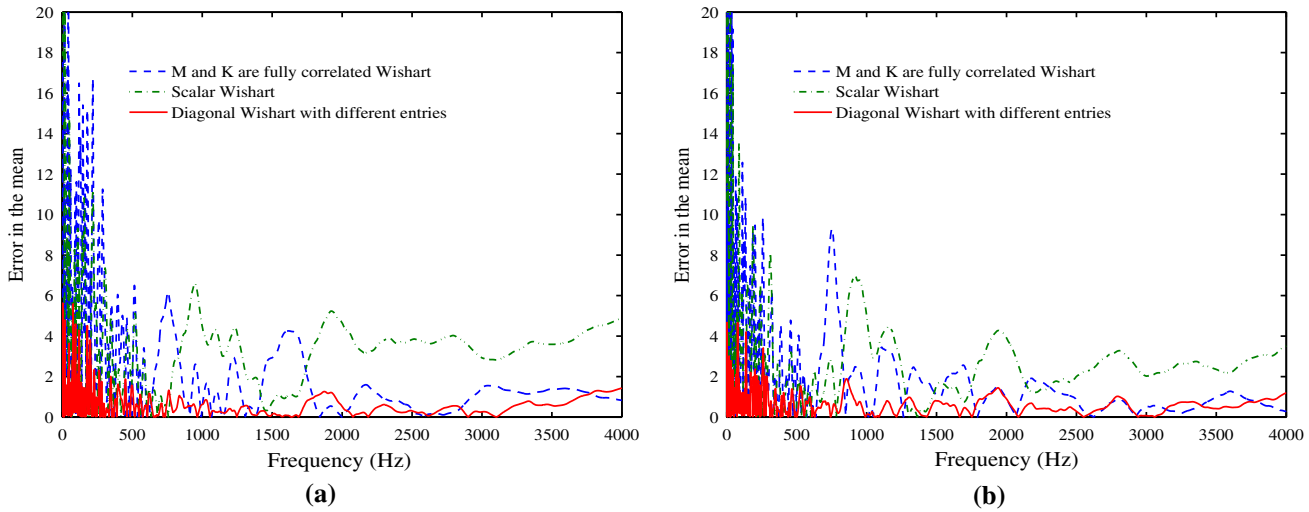

Fig. 3 Comparison of percentage errors in the mean of the amplitude obtained using the three Wishart matrix approaches for the plate with randomly inhomogeneous material properties. **a** Driving-point-FRF. **b** Cross FRF

5.2 Plate with randomly attached spring-mass oscillators: nonparametric uncertainty problem

In this example we consider the same plate but with non-parametric uncertainty. The baseline model is perturbed by attaching ten spring mass oscillators with random natural frequencies at random nodal points in the plate. The natural frequencies of the attached oscillators follow a uniform distribution between 0.2 and 4.0 kHz. The nature of uncertainty in this case is different from the previous case because here the sparsity structure of the system matrices change with different realizations of the system. Again a 5000-sample Monte Carlo simulation is performed to obtain the FRFs. From the simulated random mass and stiffness matrices we obtain $\delta_M = 0.1326$ and $\delta_K = 0.4201$. Since 2% constant modal damping factor is assumed for all the modes, $\delta_C = 0$. The *only* uncertainty related information used in the random matrix approach are the values of δ_M and δ_K. The information regarding the location and natural frequencies of the attached oscillators are *not* used in the Wishart matrix approach. This is aimed to depict a realistic situation when the detailed information regarding uncertainties in a complex engineering system is not available to the analyst.

The predicted mean of the amplitude using the direct Monte Carlo simulation and three Wishart matrix approaches are compared in Fig. 6 for the driving-point-FRF (node number 481) and a cross FRF (node number 877). In Fig. 7, percentage errors in the mean of the amplitude of the driving-point and cross-FRF obtained using the proposed three Wishart matrix approaches are shown. Percentage errors are

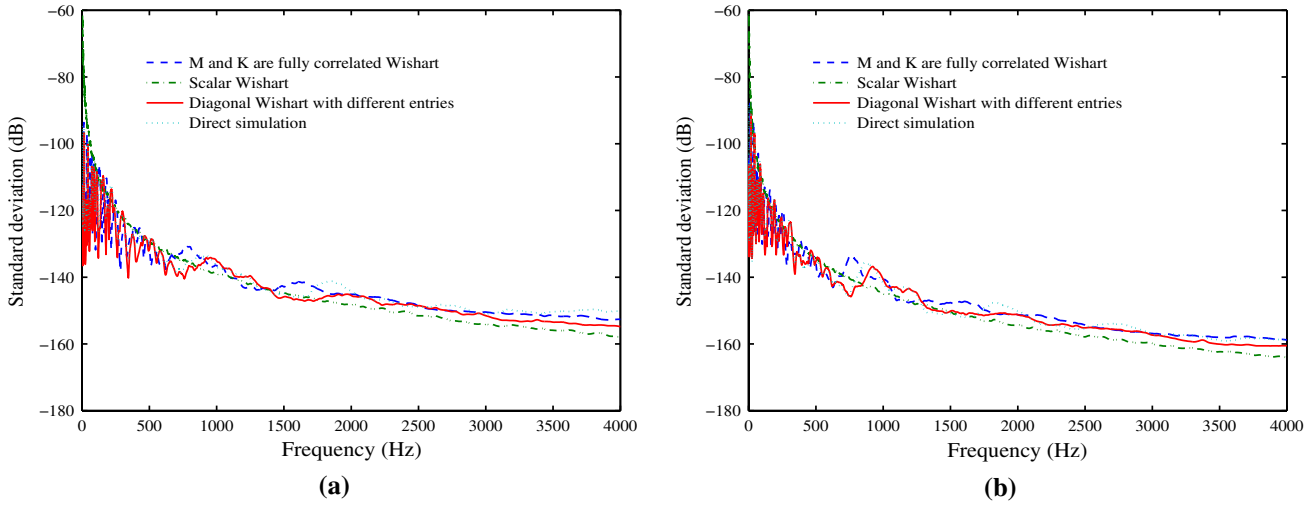

Fig. 4 Comparison of the standard deviation of the amplitude obtained using the direct stochastic finite element simulation and three Wishart matrix approaches for the plate with randomly inhomogeneous material properties. **a** Driving-point-FRF. **b** Cross FRF

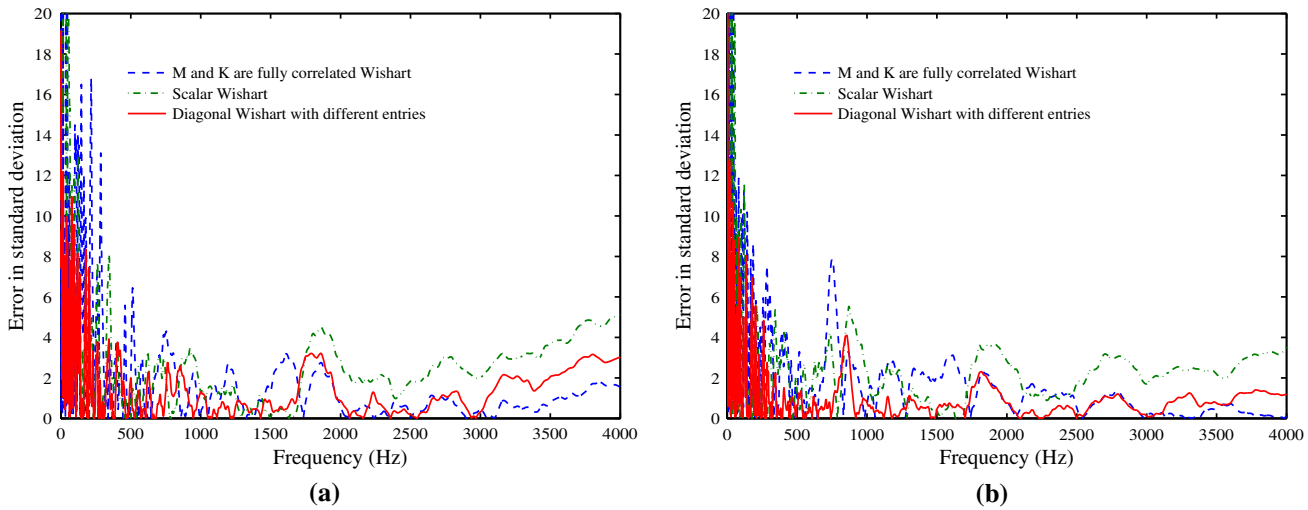

Fig. 5 Comparison of percentage errors in the standard deviation of the amplitude obtained using the three Wishart matrix approaches for the plate with randomly inhomogeneous material properties. **a** Driving-point-FRF. **b** Cross FRF

calculated using the direct Monte Carlo simulation results as the benchmarks.

The predicted standard deviation of the amplitude using the direct Monte Carlo simulation and three Wishart matrix approaches are compared in Fig. 8 for the driving-point and cross-FRF. In Fig. 9 percentage errors in the standard deviation of the amplitude of the driving-point and cross-FRF obtained using the proposed three Wishart matrix approaches are shown. Percentage errors are calculated using the direct Monte Carlo simulation results as the benchmarks. Like the previous example with parametric uncertainty, error using any one of the random matrix approaches reduce with the increase in frequency. Among the three Wishart matrix approaches discussed here, the diagonal Wishart matrix with different entries produces most accurate results across the frequency range. Note that this approach only need the simulation of one random matrix. From these results we conclude that the diagonal Wishart matrix with different entries should be used for a system with nonparametric uncertainty as well. In the next section we discuss the application of the proposed approach in the context of a physical experiment.

6 Experimental validation

We consider the dynamics of a steel cantilever plate with homogeneous geometric (i.e. uniform thickness) and constitutive properties (i.e. uniform Young's modulus and Poisson's ratio). This uniform plate defines (as considered in the numerical studies in the previous section) the baseline system. The

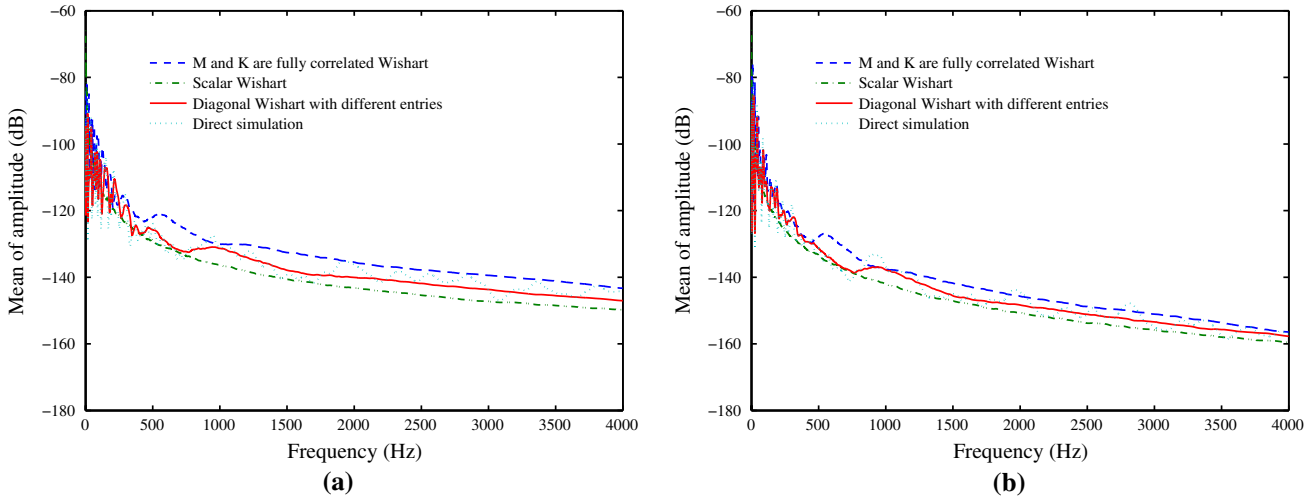

Fig. 6 Comparison of the mean of the amplitude obtained using the direct stochastic finite element simulation and three Wishart matrix approaches for the plate with randomly attached oscillators. **a** Driving-point-FRF. **b** Cross FRF

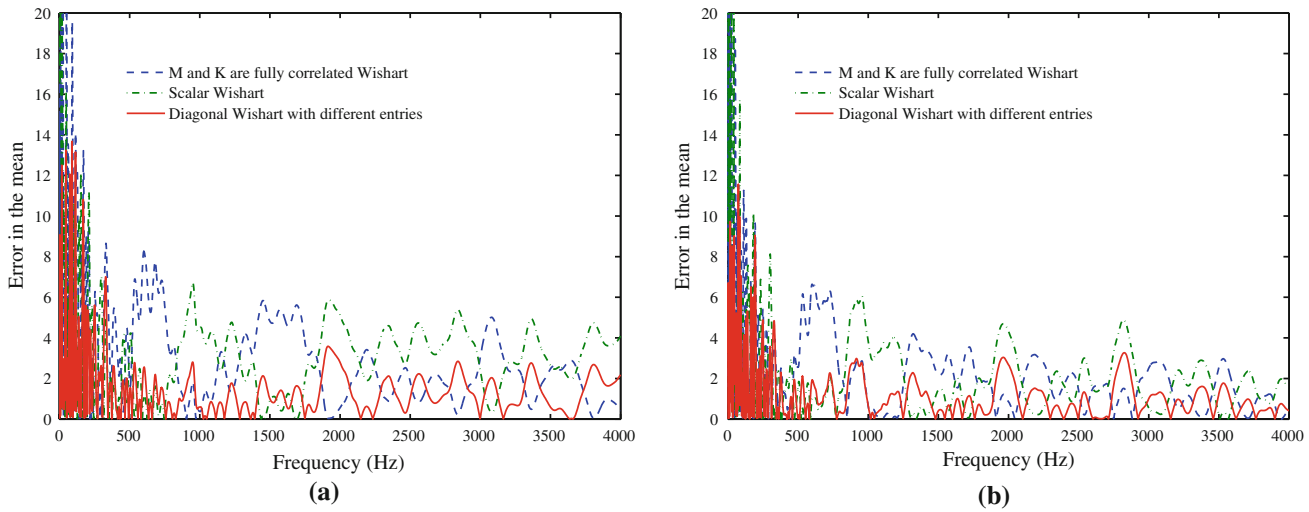

Fig. 7 Comparison of percentage errors in the mean of the amplitude obtained using the three Wishart matrix approaches for the plate with randomly attached oscillators. **a** Driving-point-FRF. **b** Cross FRF

baseline model is perturbed by a set of spring-mass oscillators with different natural frequencies and attached randomly along the plate. Here we investigate the feasibility of adopting the proposed simplified random matrix model for this case.

6.1 Overview of the experiential method

The details of this experiment has been described by Adhikari et al. [10,12]. Here we give a very brief overview. The test rig has been designed for simplicity and ease of replication and modelling. The overall arrangement of the test-rig is shown in Fig. 10. A rectangular steel plate with uniform thickness is used for the experiment. The physical and geometrical properties of the steel plate are shown in Table 1. The plate is clamped along one edge using a clamping device. The clamping device is attached on the top of a heavy concrete block and the whole assembly is placed on a steel table. The plate weights about 12.28 kg and special care has been taken to ensure its stability and minimizing the vibration transmission. The plate is 'divided' into 375 elements (25 along the length and 15 along the width). Assuming one corner on the cantilevered edge as the origin, we have assigned co-ordinates to all the nodes. Oscillators and accelerometers are attached on these nodes. This has been done with the view of easy finite element modeling. The bottom surface of the plate is marked with node numbers so that the oscillators can be hung at the nodal locations. This scheme is aimed at reducing uncertainly arising from the measurement of the locations of the oscillators. A discrete random number

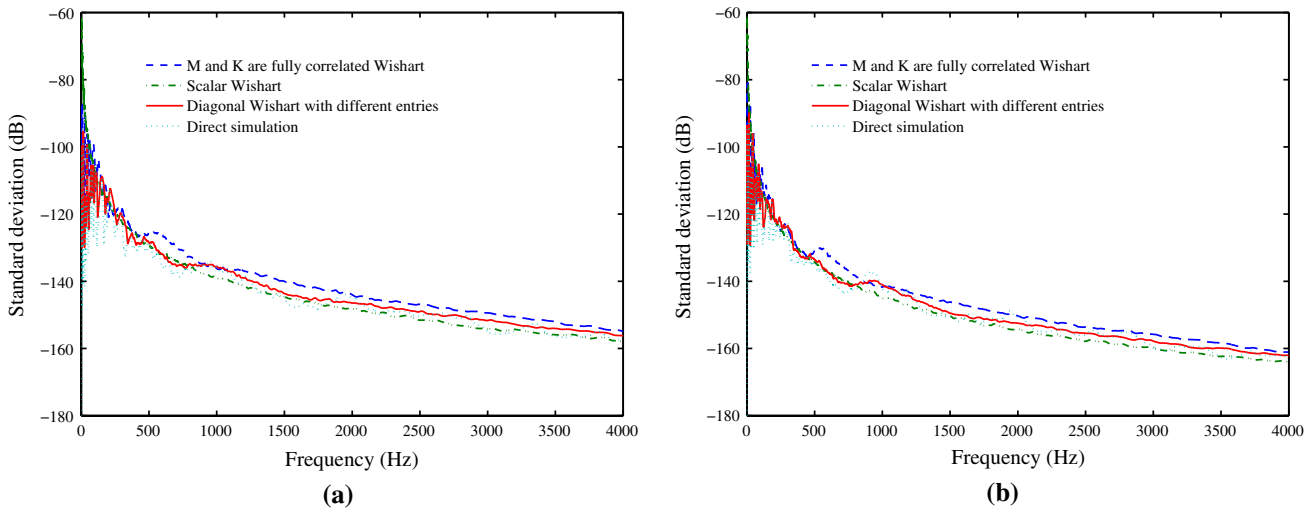

Fig. 8 Comparison of the standard deviation of the amplitude obtained using the direct stochastic finite element simulation and three Wishart matrix approaches for the plate with randomly attached oscillators. **a** Driving-point-FRF. **b** Cross FRF

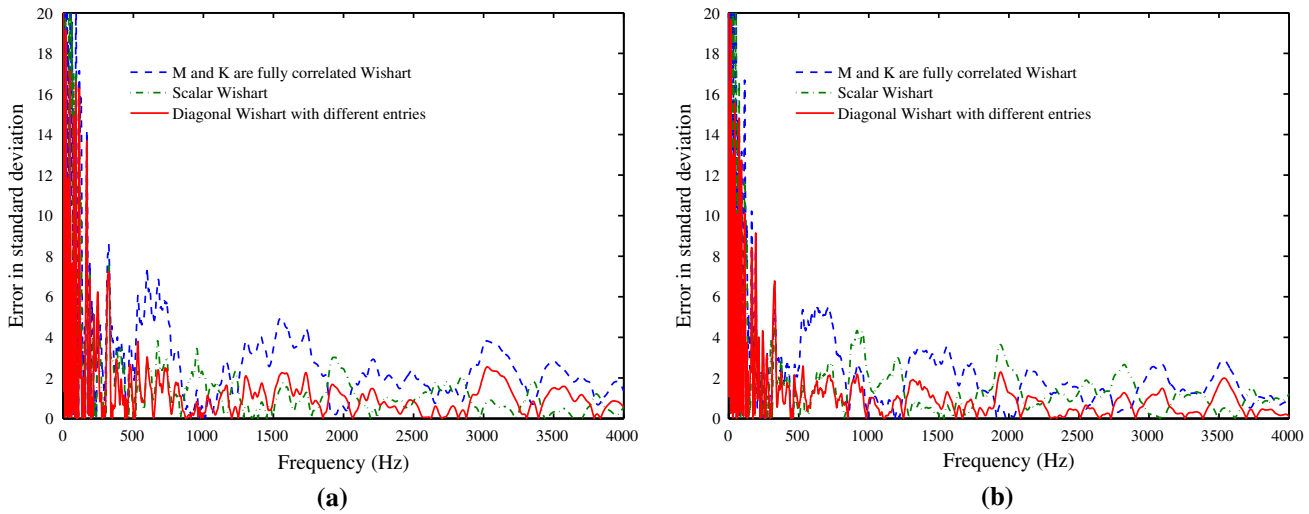

Fig. 9 Comparison of percentage errors in the standard deviation of the amplitude obtained using the three Wishart matrix approaches for the plate with randomly attached oscillators. **a** Driving-point-FRF. **b** Cross FRF

generator is used to generate the X and Y coordinates of the oscillators. In total ten oscillators are used to simulate random unmodelled dynamics. The spring is glue-welded with a magnet at the top and a mass at the bottom. The magnet at the top of the assembly helps to attach the oscillators at the bottom of the plate repeatedly without much difficulty. The stiffness of the ten springs used in the experiments is given in Table 2. In the same table we have also shown the natural frequency of the individual oscillators. The oscillating mass of each of the ten oscillators is 121.4 g. Therefore the total oscillating mass is 1.214 Kg, which is 9.8% of the mass of the plate. The springs are attached to the plate at the pre-generated nodal locations using the small magnets located at the top the assembly. The small magnets (weighting 2 g) are found to be strong enough to hold the 121.4 g mass attached to the spring below over the frequency range considered. A sample realization of the of the attached oscillators is shown in Fig. 10b. One hundred such realizations of the oscillators are created (by hanging the oscillators at random locations) and tested individually in this experiment.

A 32 channel LMS™ system and a shaker is employed to perform the modal analysis [16,24,43]. We used the shaker to act as an impulse hammer. The shaker was placed so that it impacted at the (4,6) node of the plate. The shaker was driven by a signal from a Simulink™ and dSpace™ system via a power amplifier. The problem with using the usual manual hammer is that it is in general difficult to hit the bottom of the plate exactly at the same point with the same amount of force for every sample run. The shaker generates impulses at a pulse rate of 20 s and a pulse width of 0.01 s. Using the

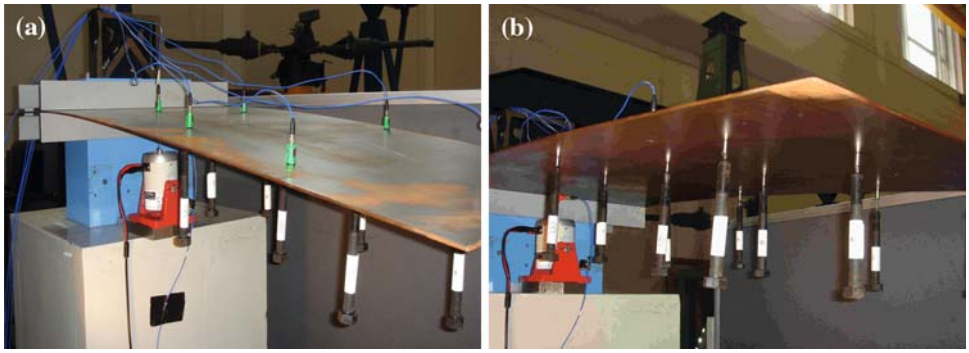

Fig. 10 The test rig for the cantilever plate. The position of the shaker (used as a impact hammer) and the accelerometers are shown in the sub-figure (**a**). A sample of attached oscillators at random locations is shown in sub-figure (**b**). The spring stiffness varies so that the oscillator frequencies are between 43 and 70 Hz

Table 1 Material and geometric properties of the cantilever plate considered for the experiment

Plate Properties	Numerical values
Length (L)	998 mm
Width (b)	530 mm
Thickness (t_h)	3.0 mm
Mass density (ρ)	7,800 kg/m^3
Young's modulus (E)	2.0×10^5 MPa
Total weight	12.38 kg

Table 2 Stiffness of the springs and natural frequency of the oscillators used to simulate unmodelled dynamics (the mass of the each oscillator is 121.4 g)

Oscillator number	Spring stiffness ($\times 10^4$ N/m)	Natural frequency (Hz)
1	1.6800	59.2060
2	0.9100	43.5744
3	1.7030	59.6099
4	2.4000	70.7647
5	1.5670	57.1801
6	2.2880	69.0938
7	1.7030	59.6099
8	2.2880	69.0938
9	2.1360	66.7592
10	1.9800	64.2752

shaker in this way we have tried to eliminate any uncertainties arising from the input forces. Six accelerometers are used as the response sensors. The locations of the six sensors are selected such that they cover a broad area of the plate. The locations of the accelerometers can be seen in Fig. 10. The nodal locations of the accelerometers are as follows: Point 1: (4,6), Point 2: (6,11), Point 3: (11,3), Point 4: (14,14), Point 5: (18,2), Point 6: (21,10). Note that these are the same points used in the simulation study in the previous section. Small holes are drilled into the plate and all of the six accelerometers are attached by screwing through the holes. The signal from the force transducer is amplified using an amplifier while the signals from the accelerometers are directly input into the LMS system. For data acquisition and processing, LMS Test Lab 5.0 is used. In the Impact Scope, we have set the bandwidth to 8,192 Hz with 8,192 spectral lines (i.e., 1.00 Hz resolution). Five averages are taken for each FRF measurement.

6.2 Comparison with experiential results

The mean of the amplitude from experiment and three Wishart matrix approaches are compared in Fig. 11 for the driving-point-FRF (point 1) and a cross FRF (point 2). In the numerical calculations with Wishart matrices 375 elements are used and the resulting finite element model has 1,200 degrees-of-freedom. We have used 2,000 samples in the Monte Carlo simulations. A modal damping factor of 0.7% is assumed for all of the modes. A constant damping factor for all the modes is an assumption. Ideally one should identify modal damping factors for all possible modes and perhaps take an average over the 100 realizations in the experiment. It is however a widely established practice to treat damping in a simple manner such as a constant modal damping factor as considered here. This study also verifies if such ad-hoc assumptions on damping can produce any meaningful predictions.

Recall that there are four key parameters needed to implement the random matrix approach. They are respectively the mean and normalized standard deviation of the mass and stiffness matrices. The mean system is considered to be the cantilever plate shown in Fig. 1 discussed in the previous section. The mean mass and stiffness matrices are obtained using the

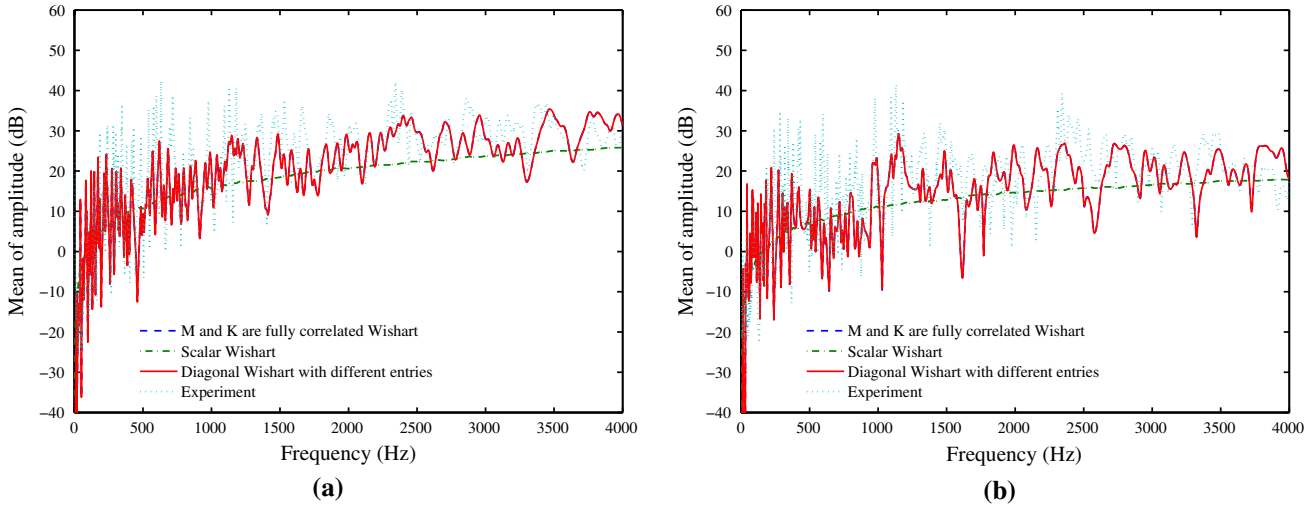

Fig. 11 Comparison of the mean of the amplitude obtained using the experiment and three Wishart matrix approaches for the plate with randomly attached oscillators. **a** Driving-point-FRF. **b** Cross FRF

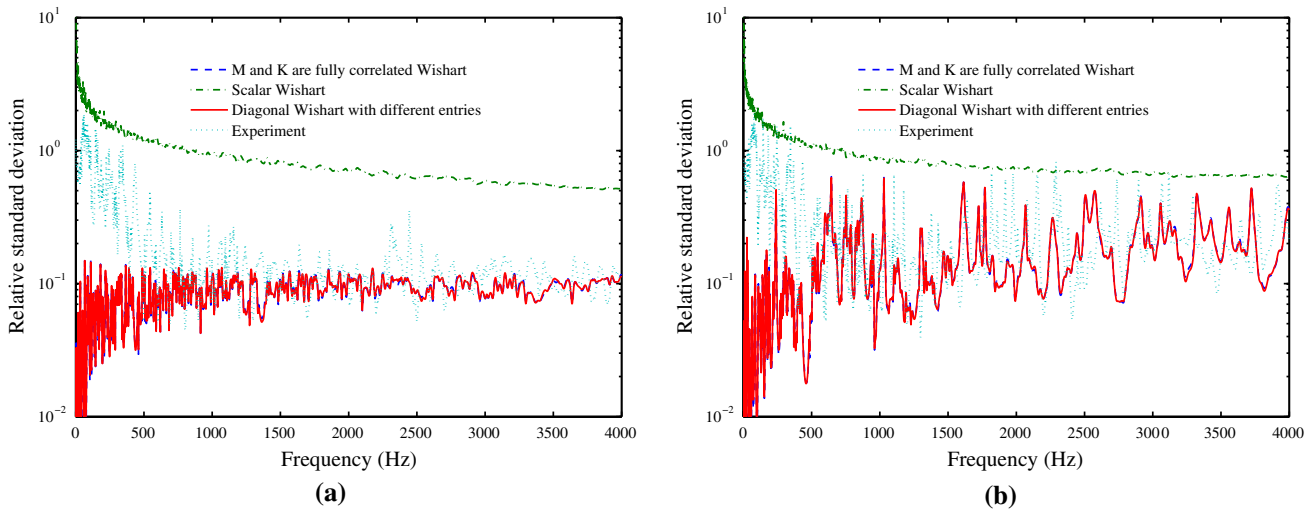

Fig. 12 Comparison of relative standard deviation of the amplitude obtained using the experiment and three Wishart matrix approaches for the plate with randomly attached oscillators. **a** Driving-point-FRF. **b** Cross FRF

standard finite element approach. The mean damping matrix for the experimental system is not obtained explicitly as constant modal damping factors are used. All 100 realizations of the plate and oscillators were individually simulated. Then the samples of $1{,}200 \times 1{,}200$ mass and stiffness matrices were stored. Normalized standard deviation (the dispersion parameters) of the mass and stiffness matrices are obtained as $\delta_M = 0.0286$ and $\delta_K = 0.0017$. The *only* uncertainty related information used in the random matrix approach are the values of δ_M and δ_K. The explicit information regarding the spatial locations of the attached oscillators including their stiffness and mass properties are *not* used in fitting the Wishart matrices. This is aimed to depict a realistic situation when the detailed information regarding uncertainties in a complex engineering system is not available to the analyst.

In Fig. 11, observe that the results from the scalar Wishart model is qualitatively different from the other two approaches. In that the mean response curve is very smooth and very little 'fluctuations' can be seen. The results obtained using the fully correlated **M** and **K** Wishart matrices and the diagonal Wishart matrix with different entries are almost similar. Qualitatively these simulation results agree well with the experimental results. The discrepancies, especially in the low frequency regions, are perhaps due to incorrect values of the damping factors. The relative standard deviation of the amplitude from experiment and three Wishart matrix approaches are compared in Fig. 12 for the driving-point-FRF and the cross FRF. We obtained the relative standard deviation by dividing the standard deviation with the respective mean values. This is done in an attempt to eliminate the effect of

damping on the mean values and consider the variability only. As expected, the predictions using the Wishart random matrix models in the lower frequency ranges are not very accurate. Like the mean predictions, the results using the scalar Wishart random matrix turns out to be most inaccurate. The other two approaches are very similar and in the higher frequencies they agree well with the experimental results.

7 Summary of the computational approach

From the numerical and experimental studies conducted so far it can be concluded that the generalized Wishart matrix with different diagonal entries is the best random matrix model when both accuracy and computational efficiency are considered. Numerical calculations for 5000 samples and with 1,200 × 1,200 matrix size show that is it about 30% less computationally expensive compared to fully correlated mass and stiffness Wishart matrices. The relative computational efficiency is likely to increase for larger system sizes and increasing samples. This new approach leads to a simple and general simulation algorithm for probabilistic structural dynamics. A step-by-step method for implementing the new computational approach in conjunction with general purpose finite element software is given below:

1. Form the deterministic mass and stiffness matrices $\mathbf{M}_0$ and $\mathbf{K}_0$ using the standard finite element method. Obtain n, the dimension of the system matrices and the modal damping factors ζ_j.
2. Solve the deterministic undamped eigenvalue problem

$$\mathbf{K}_0\boldsymbol{\phi}_{0j} = \omega_{0_j}^2\mathbf{M}_0\boldsymbol{\phi}_{0j}, \quad j = 1, 2, \ldots, n \tag{60}$$

and create the matrix

$$\boldsymbol{\Phi}_0 = \left[\boldsymbol{\phi}_{0_1}, \boldsymbol{\phi}_{0_2}, \ldots, \boldsymbol{\phi}_{0_n}\right] \tag{61}$$

Calculate the ratio

$$\gamma_H = \left(\sum_{j=1}^{n}\omega_{0_j}^2\right)^2 / \sum_{j=1}^{n}\omega_{0_j}^4 \tag{62}$$

3. Obtain the dispersion parameters δ_M and δ_K corresponding to the mass and stiffness matrices. This can be obtained from physical or computer experiments.
4. Calculate the scalar constants

$$p_1 = \frac{1}{\delta_M^2}\left\{1 + \{\text{Trace}\,(\mathbf{M}_0)\}^2/\text{Trace}\left(\mathbf{M}_0{}^2\right)\right\} \quad \text{and}$$
$$p_2 = \frac{1}{\delta_K^2}\left\{1 + \{\text{Trace}\,(\mathbf{K}_0)\}^2/\text{Trace}\left(\mathbf{K}_0{}^2\right)\right\} \tag{63}$$

5. Obtain the dispersion parameter of the generalized Wishart matrix

$$\delta_H = \frac{\left({p_1}^2+(p_2-2-2n)\,p_1+(-n-1)\,p_2+n^2+1+2n\right)\gamma_H}{p_2\,(-p_1+n)\,(-p_1+n+3)} + \frac{{p_1}^2+(p_2-2n)\,p_1+(1-n)\,p_2-1+n^2}{p_2\,(-p_1+n)\,(-p_1+n+3)} \tag{64}$$

6. Calculate the parameters

$$\theta = \frac{(1+\gamma_H)}{\delta_H^2} - (n+1) \quad \text{and} \quad p = [n+1+\theta] \tag{65}$$

where p is approximated to the nearest integer of $n + 1 + \theta$.
7. Create an $n \times p$ matrix $\mathbf{Y}$ such that

$$Y_{ij} = \omega_{0_i}\widetilde{Y}_{ij}/\sqrt{\theta}; \quad i = 1, 2, \ldots, n; \quad j = 1, 2, \ldots, p \tag{66}$$

where $\widetilde{Y}_{ij}$ are independent and identically distributed (i.i.d.) Gaussian random numbers with zero mean and unit standard deviation.
8. Form the $n \times n$ matrix

$$\boldsymbol{\Xi} = \mathbf{Y}\mathbf{Y}^T \quad \text{or} \quad \Xi_{ij} = \frac{\omega_{0_i}\omega_{0_j}}{\theta}\sum_{k=1}^{p}\widetilde{Y}_{ik}\widetilde{Y}_{jk}; \quad i = 1, 2, \ldots, n; \quad j = 1, 2, \ldots, n \tag{67}$$

and solve the symmetric eigenvalue problem for every sample

$$\boldsymbol{\Xi}\,\boldsymbol{\Psi}_r = \boldsymbol{\Omega}_r^2\boldsymbol{\Psi}_r, \quad \forall r = 1, 2, \ldots, n_{\text{samp}} \tag{68}$$

9. Obtain the eigenvector matrix

$$\mathbf{X}_r = \boldsymbol{\Phi}_0\boldsymbol{\Psi}_r \tag{69}$$

and calculate the dynamic response in the frequency domain as

$$\bar{\mathbf{q}}_r(\mathrm{i}\omega) = \sum_{j=1}^{n}\frac{\mathbf{x}_{r_j}^T\bar{\mathbf{f}}(s)}{-\omega^2 + 2\mathrm{i}\omega\zeta_j\omega_{r_j} + \omega_{r_j}^2}\mathbf{x}_{r_j} \tag{70}$$

The above procedure can be implemented very easily. When one implements this approach in conjunction with a general purpose commercial finite element software, the commercial software needs to be accessed only once to obtain the mean matrices $\mathbf{M}_0$ and $\mathbf{K}_0$ and solve the corresponding deterministic eigenvalue problem. This computational procedure proposed here is therefore 'non-intrusive' and can be used consistently across the frequency ranges [38].

8 Conclusions

When uncertainties in the system parameters and modelling are considered, the discretized equation of motion of linear dynamical systems is characterized by random mass, stiffness and damping matrices. The possibility of using a single Wishart random matrix model for the system is investigated in the paper. Closed-form analytical expressions of the parameters of the Wishart random matrices have been derived using the theory of matrix variate distributions. The proposed Wishart random matrix models are applied to the forced vibration problem of a plate with stochastically inhomogeneous properties and randomly attached oscillators. For both cases it is possible to predict the variation of the dynamic response using the Wishart matrices across a wide range of driving frequency.

The feasibility of adopting a single Wishart random matrix model to quantify uncertainty in structural dynamical systems has also been investigated using experimental data. In particular, model uncertainty in a vibrating plate due to disorderly attached spring-mass oscillators with random natural frequencies is considered. One hundred nominally identical dynamical systems were statistically generated and individually tested in a laboratory setup. Special measures were taken so that the uncertainty in the response of the main structure primarily emerges from the random attachment configurations of the subsystems having random natural frequencies. Six frequency response functions up to 4 kHz were measured for each of the 100 tests. Two of these frequency response functions were used to understand the applicability of the proposed approach. The main conclusions based on the numerical and experimental studies conducted are:

- The simulation of separate Wishart matrices corresponding to the mass and stiffness matrices may not be necessary. Instead, it is possible to use a generalized Wishart matrix to predict the response variability. This is not only computationally efficient, but can also give insights into the distribution of the eigenvalues of the system.
- Two new generalized Wishart matrix models, namely (1) generalized scalar Wishart distribution and (2) generalized diagonal Wishart distribution have been proposed and investigated. Model ‘a’ is very simple but inaccurate in the lower frequency ranges. Model ‘b’ turns out to be the most accurate across the frequency range.
- Considering that the available information is the mean and (normalized) standard deviation of mass and stiffness matrices, three different approaches are compared for problem with parametric uncertainty and non-parametric uncertainty. It is shown that for model ‘b’, that is the generalized diagonal Wishart distribution, the calculated response statistics are in best agreements with the direct numerical simulation and experimental results.
- Numerical as well as experimental results show that the difference between three proposed approaches are more in the low frequency regions and less in the higher frequency regions.

These results suggest that a generalized diagonal Wishart distribution with suggested parameters may be used as a consistent and unified uncertainty quantification tool.

Acknowledgments The author gratefully acknowledges the support of UK Engineering and Physical Sciences Research Council (EPSRC) through the award of an Advanced Research Fellowship and The Leverhulme Trust for the award of the Philip Leverhulme Prize.

References

1. Adhikari S (1999) Modal analysis of linear asymmetric non-conservative systems. ASCE J Eng Mech 125(12):1372–1379
2. Adhikari S (2004) Optimal complex modes and an index of damping non-proportionality. Mech Syst Signal Process 18(1):1–27
3. Adhikari S (2005) Qualitative dynamic characteristics of a non-viscously damped oscillator. Proc R Soc London Ser A 461(2059):2269–2288
4. Adhikari S (2006) Damping modelling using generalized proportional damping. J Sound Vib 293(1–2):156–170
5. Adhikari S (2007) Matrix variate distributions for probabilistic structural mechanics. AIAA J 45(7):1748–1762
6. Adhikari S (2007) On the quantification of damping model uncertainty. J Sound Vib 305(1–2):153–171
7. Adhikari S (2008) Wishart random matrices in probabilistic structural mechanics. ASCE J Eng Mech 134(12):1029–1044
8. Adhikari S, Manohar CS (1999) Dynamic analysis of framed structures with statistical uncertainties. Int J Numer Methods Eng 44(8):1157–1178
9. Adhikari S, Manohar CS (2000) Transient dynamics of stochastically parametered beams. ASCE J Eng Mech 126(11):1131–1140
10. Adhikari S, Sarkar A (2009) Uncertainty in structural dynamics: experimental validation of wishart random matrix model. J Sound Vib 323(3–5):802–825
11. Adhikari S, Wagner N (2004) Direct time-domain approach for exponentially damped systems. Comput Struct 82(29–30): 2453–2461
12. Adhikari S, Friswell MI, Lonkar K, Sarkar A (2009) Experimental case studies for uncertainty quantification in structural dynamics. Probab Eng Mech 24(4):473–492
13. Caughey TK, O’Kelly MEJ (1965) Classical normal modes in damped linear dynamic systems. Trans ASME/J Appl Mech 32:583–588
14. Eaton ML (1983) Multivariate statistics: a vector space approach. Wiley, New York
15. Elishakoff I, Ren YJ (2003) Large variation finite element method for stochastic problems. Oxford University Press, Oxford
16. Ewins DJ (2000) Modal testing: theory and practice, 2nd edn. Research Studies Press, Baldock
17. Ghanem R, Spanos P (1991) Stochastic finite elements: a spectral approach. Springer, New York
18. Girko VL (1990) Theory of random determinants. Kluwer, The Netherlands
19. Gupta A, Nagar D (2000) Matrix variate distributions. In: Monographs and surveys in pure and applied mathematics. Chapman & Hall, London

20. Haldar A, Mahadevan S (2000) Reliability assessment using stochastic finite element analysis. Wiley, New York
21. Hanson KM, Hemez FM (2001) A framework for assessing confidence in computational predictions—computational validation series: part 3. Exp Tech 25(4):50–55
22. Hemez FM (2004) Uncertainty quantification and the verification and validation of computational models. In: Inman DJ, Farrar CR, Junior VL, Junior VS (eds) Damage prognosis for aerospace. Civil and Mechanical Systems, Wiley, London
23. Kleiber M, Hien TD (1992) The stochastic finite element method. Wiley, Chichester
24. Maia NMM, Silva JMM (eds) (1997) Theoretical and experimental modal analysis. In: Robetrs JB (ed) Engineering dynamics series. Research Studies Press, Taunton
25. Manohar CS, Adhikari S (1998) Dynamic stiffness of randomly parametered beams. Probab Eng Mech 13(1):39–51
26. Manohar CS, Adhikari S (1998) Statistical analysis of vibration energy flow in randomly parametered trusses. J Sound Vib 217(1):43–74
27. Mathai AM, Provost SB (1992) Quadratic forms in random variables: theory and applications. Marcel Dekker, New York
28. Matthies HG, Brenner CE, Bucher CG, Soares CG (1997) Uncertainties in probabilistic numerical analysis of structures and solids—stochastic finite elements. Struct Safety 19(3):283–336
29. Meirovitch L (1997) Principles and techniques of vibrations. Prentice-Hall, New Jersey
30. Mezzadri F, Snaith NC (eds) (2005) Recent perspectives in random matrix theory and number theory. In: London Mathematical Society lecture note. Cambridge University Press, Cambridge
31. Mignolet MP, Soize C (2008) Nonparametric stochastic modeling of linear systems with prescribed variance of several natural frequencies. Probab Eng Mech 23(2–3):267–278
32. Mignolet MP, Soize C (2008) Stochastic reduced order models for uncertain geometrically nonlinear dynamical systems. Comput Methods Appl Mech Eng 197(45–48):3951–3963
33. Muirhead RJ (1982) Aspects of multivariate statistical theory. Wiley, New York
34. Nair PB, Keane AJ (2002) Stochastic reduced basis methods. AIAA J 40(8):1653–1664
35. Oberkampf WL, Barone MF (2006) Measures of agreement between computation and experiment: validation metrics. J Comput Phys 217(1):5–36
36. Papoulis A, Pillai SU (2002) Probability, random variables and stochastic processes, 4th edn. McGraw-Hill, Boston
37. Pellissetti M, Capiez-Lernout E, Pradlwarter H, Soize C, Schueller GI (2008) Reliability analysis of a satellite structure with a parametric and a non-parametric probabilistic model. Comput Methods Appl Mech Eng 198(2):344–357
38. Pradlwarter HJ, Schuëller GI (2005) A consistent concept for high- and low-frequency dynamics based on stochastic modal analysis. J Sound Vib 288(3):653–667
39. Rayleigh L (1877) Theory of sound (two volumes), 1945th edn. Dover, New York
40. Sachdeva SK, Nair PB, Keane AJ (2006) Comparative study of projection schemes for stochastic finite element analysis. Comput Methods Appl Mech Eng 195(19–22):2371–2392
41. Sachdeva SK, Nair PB, Keane AJ (2006) Hybridization of stochastic reduced basis methods with polynomial chaos expansions. Probab Eng Mech 21(2):182–192
42. Shinozuka M, Yamazaki F (1998) Stochastic finite element analysis: an introduction. In: Ariaratnam ST, Schuëller GI, Elishakoff I (eds) Stochastic structural dynamics: progress in theory and applications. Elsevier, London
43. Silva JMM, Maia NMM (eds) (1998) Modal analysis and testing. In: Proceedings of the NATO Advanced Study Institute, NATO Science Series: E: Applied Science, Sesimbra, Portugal
44. Soize C (2000) A nonparametric model of random uncertainties for reduced matrix models in structural dynamics. Probab Eng Mech 15(3):277–294
45. Soize C (2001) Maximum entropy approach for modeling random uncertainties in transient elastodynamics. J Acoust Soc Am 109(5):1979–1996
46. Soize C (2005) Random matrix theory for modeling uncertainties in computational mechanics. Comput Methods Appl Mech Eng 194(12–16):1333–1366
47. Soize C, Capiez-Lernout E, Durand JF, Fernandez C, Gagliardini L (2008a) Probabilistic model identification of uncertainties in computational models for dynamical systems and experimental validation. Comput Methods Appl Mech Eng 198(1, Sp. Iss. SI):150–163
48. Soize C, Capiez-Lernout E, Ohayon R (2008b) Robust updating of uncertain computational models using experimental modal analysis. AIAA J 46(11):2955–2965
49. Sudret B, Der-Kiureghian A (2000) Stochastic finite element methods and reliability. Technical Report UCB/SEMM-2000/08, Department of Civil and Environmental Engineering, University Of California, Berkeley
50. Tulino AM, Verdú S (2004) Random matrix theory and wireless communications. Now Publishers Inc., Hanover, MA, USA